

1
2 **Role of interface reaction on resistive switching**
3 **of Metal/*a*-TiO₂/Al RRAM devices**
4
5

6
7 Hu Young Jeong and Jeong Yong Lee^{a)}

8 *Department of Materials Science and Engineering, KAIST, Daejeon 305-701, Korea*

9 Sung-Yool Choi^{b)}

10 *Electronics and Telecommunications Research Institute (ETRI)*

11 *161 Gajeong-Dong, Yuseong-Gu, Daejeon, 305-700, Korea*
12
13
14

15 For the clear understanding of the role of interface reaction between top metal
16 electrode and titanium oxide layer, we investigated the effects of various top metals on the
17 resistive switching in Metal/*a*-TiO₂/Al devices. The top Al device with the highest oxygen
18 affinity showed the best memory performance, which is attributed to the fast formation of
19 interfacial layer (Al-Ti-O), as confirmed by high resolution transmission electron
20 microscopy and electron dispersive spectroscopy. Hence, we concluded that the interface
21 layer, created by the redox reaction between top metal electrode and TiO₂ layer, plays a
22 crucial role in bipolar resistive switching behaviors of metal/TiO₂/Al systems.
23

^{a)} Electronic mail: j.y.lee@kaist.ac.kr

^{b)} Electronic mail: sychoi@etri.re.kr

1 Recently, binary transition metal oxides such as NiO,¹ TiO₂,² and ZnO,³ have
2 attracted a great deal of interest as high potential next-generation nonvolatile memory
3 (NVM) due to their simple device structure, easy fabrication process and high CMOS
4 compatibility. For the advanced development of actual RRAM devices, the clear
5 understanding of the basic mechanism is essential, but the driving mechanism of the
6 resistance switching behaviors remains controversial. To clarify the underlying mechanism,
7 many researchers have studied intensively the microscopic origins of the resistive
8 switching in binary oxide films.^{4,5} In particular, the effects of various metal electrodes on
9 the resistive switching of various binary oxide thin films such as NiO⁶ and ZrO₂⁷ have been
10 investigated to identify the role of interface. However, there exist few works regarding the
11 role of the interface between an amorphous TiO₂ film and the top metal electrodes.

12 In this letter, we report the influence of top metal electrodes on the resistive
13 switching properties in Metal/TiO₂/Al devices with the several kinds of metallic electrode
14 such as Al, Cr, Mo, W, and Pt in order to support our resistive driving model. In the case of
15 Al top electrode, which has the lowest oxide formation energy, the largest hysteresis and
16 highest on/off ratio were shown among the tested device structures. It can be strongly
17 confirmed that the resistive switching behavior is deeply related with the interface reaction
18 between top metal electrode and titanium oxide layer.

19 Amorphous TiO₂ films were deposited on Al/SiO₂/Si substrates by plasma-enhanced
20 atomic layer deposition (PEALD) methods.^{8,9} During the deposition process (200cycle),
21 substrate temperature was kept at 180 °C. Titanium tetra-iso-propoxide (TTIP) and oxygen
22 plasma were used as the Ti and oxygen precursors, respectively. The aluminum electrodes
23 with a thickness of 60nm were deposited by thermal evaporation method, forming the
24 cross-bar type structures using a metal shadow mask with a line width of 60 μm, as shown
25 in the right inset of Fig. 1(a). In order to investigate the electrical properties of amorphous

1 titanium oxide films with several different metals, metal top electrodes (Al, Cr, Mo, W, and
2 Pt) were deposited by thermal evaporation, e-beam evaporation, and RF magnetron
3 sputtering methods. The electrical property (I-V curve) was measured using a Keithley
4 4200 Semiconductor Characterization System in a dc sweep mode. The cross-sectional
5 HR-TEM images of Metal/TiO₂/Al samples were examined using a 300 kV JEOL JEM
6 3010 with a 0.17 nm point resolution. Annular dark field (ADF) scanning TEM (STEM)
7 image and point energy dispersive x-ray spectroscopy (EDS) data were obtained using
8 field emission transmission electron microscope (Tecnai G2 F30) equipped with STEM
9 mode and an EDS analyzer.

10 Figure 1 shows the typical J-V curves of Metal/TiO₂/Al memory cells with Al, Cr,
11 Mo, W, and Pt electrodes, which were measured in a voltage region (-4V~ 4V) under the
12 dc voltage sweep. A Pt/TiO₂/Al device showed an ohmic behavior at the very low-voltage
13 region (-0.1V ~ +0.1V) (data not shown here). This interesting phenomenon cannot be
14 explained by a general semiconductor concept because Pt is expected to form a Schottky-
15 like contact with the n-type semiconductor TiO₂ due to a high work function of Pt
16 (~5.65eV).¹⁰ On the other hand, a device with Al top metal of a low work function
17 (~4.28eV)¹⁰ represents the most non-ohmic behaviors, showing remarkably low current
18 level in the negative voltage region. Therefore, it can be inferred that the new factor such
19 as interface layer, which has a high resistance than TiO₂ itself, is involved in this system
20 rather than the general theory of metal-semiconductor contact. All devices showed a
21 hysteretic behavior and bipolar resistive memory switching. However, it is noted that the
22 switching voltage, the current level and On/Off ratio varied. The Al/TiO₂/Al device shows
23 considerably the highest hysteresis and On/Off ratio than any other top electrode devices,
24 supporting that the resistance change is deeply associated with the top interface reactions
25 between top electrodes and TiO₂ films.^{8,9}

1 To understand the exact conduction mechanisms, the current-voltage relationships of
2 I-V curves such as a double log plot were investigated. Figure 2(b) is the double-
3 logarithmic plots of the J-V curves for the negative voltage regions in the case of various
4 top electrodes (Al, Mo, and Pt). All devices exhibited similar I-V characteristics, which are
5 well described by the trap-controlled space-charge limited current theory, as explained in
6 our previous result.⁸ However, three remarkable differences with the change of top metal
7 electrodes are shown in the black dot-circle regions of Fig. 2(b). Firstly, in the region 2,
8 metal electrodes having large oxygen affinity like Al and Mo showed the large exponents
9 ($n \sim 4$) of V during the first negative sweep, whereas the Pt top electrode device exhibited
10 the general square law dependence ($n \sim 2$) on voltage. Secondly, the maximum slope of log
11 J-log V in the region 3, which was involved with ON/OFF ratio, increased as the oxide
12 formation energy decreased. Another important difference was also observed in the slope
13 of region 4 of the LRS. Al and Mo devices had lower values (~ 1.5) than Pt device (~ 2).
14 The reason for the differences might be attributed to the interface layer formed at the
15 vicinity of the top metal electrode during metal deposition process, as presented by our
16 earlier works.^{8,9} We suggested that the reversible formation and dissociation processes of
17 the Al-Ti-O interface by the migration of oxygen ions under an applied bias played an
18 important role in Al/a-TiO₂/Al devices. The higher slope of region 2 and 3 in the case of Al
19 indicates the formation of more insulating interface layer (Al-Ti-O), which contains a large
20 amount of oxygen ions, via the movement of oxygen ions present in bulk titanium oxide,
21 thus resulting in the steep profile of oxygen ions. The accumulated oxygen ions move back
22 to inner titanium oxide layer under the high electric field, making the device the On state.
23 On the other hand, the low value of Pt electrode device means no generation of the
24 insulating interface layer such as Pt-Ti-O. Negatively charged oxygen ions diffuse out to Pt
25 electrode due to the absence of blocking layer, thus making a slow gradient in the

1 distribution of oxygen ions at the vicinity of top interface region.

2 To directly demonstrate the abovementioned interface regions formed between
3 various top metal electrodes and titanium oxide thin films, we performed the HRTEM
4 measurements of each sample. Figure 2 is the cross-sectional HRTEM images of Al (Mo,
5 Pt)/TiO₂/Al stacked devices taken with the same magnification. Figure 2(a) shows the
6 image of the TiO₂/Al structure before the deposition of top metal electrode. Compared to
7 Fig. 2(a), after the deposition of the Al top metal, a 3-nm-thick amorphous interface layer
8 emerged, indicating the redox reaction between the Al and TiO₂ film. Compared with the
9 Al device, the samples with Mo and Pt top electrodes did not show noticeable interface
10 regions, indicating no dynamic reaction. However, it is remarkable that there was a change
11 of contrast in titanium oxide layer itself. As the oxygen affinity of top metals decreased, a
12 lighter contrast was observed, meaning the compositional change.

13 To further characterize this phenomenon, we performed a scanning TEM (STEM)
14 point energy dispersive x-ray spectroscopy (EDS) measurement. In order to effectively
15 investigate the effect of top metals, the specimens with a-TiO₂ thin films of 15 nm
16 thickness deposited on Si substrates by a PEALD method were prepared, following
17 different metal depositions (Al and Pt). For the detailed investigation of a chemical
18 composition of each titanium oxide thin layer, a point EDS analysis was conducted using a
19 STEM with a 0.7 nm probe size. Figure 4 shows annular dark field (ADF) STEM images
20 of three different samples (*a*-TiO₂/Si, Al/*a*-TiO₂/Si, and Pt/*a*-TiO₂/Si), point EDS spectra
21 measured at the region marked with red circle, and EDS line profiles scanned from a Si
22 substrate (point S) to a surface region (point F). The most striking feature was the change
23 of chemical composition of titanium oxide thin films. The atomic ratio of Ti and O, seen in
24 the right inset of Fig. 3a, b, and c, indicates that a large amount of oxygen vacancies were
25 created in the case of the Pt top electrode, which was well consistent with the EDS line

1 scan profile, as shown in Fig. 3d, e, and f. This interesting result is not agreement with the
2 general belief that the reactive metal such as Al can easily gather oxygen ions on the
3 titanium oxide layer due to highly negative oxide formation energy. Thus, in our system,
4 another model has to be considered. Schmiedl et al.¹¹ demonstrated that the grain boundary
5 diffusion of oxygen through a Pt layer of up to 17 nm is possible when the layer was
6 exposed to an air at room temperature. In a real NVM device (Pt/Ba_{0.7}Sr_{0.3}TiO₃/SRO), the
7 degradation of an endurance performance due to the diffusion of oxygen ions along the Pt
8 grain boundaries was suggested when the negative bias was applied on the Pt top
9 electrode.¹²

10 Based on these reports and our TEM results, the new schematic model to explain the
11 compositional change of titanium oxide layer according to each top electrode was
12 schematically sketched in Figure 4. In the case of the Al top electrode, the insulating layer
13 (Al-Ti-O) is rapidly formed at the initial stage of metal growth owing to a strong oxygen
14 withdrawing power of the Al metal. Because of this insulating barrier, there is no
15 additional out-diffusion of oxygen ions within the titanium oxide layer, resulting in Al-Ti-
16 O domain and corresponding *a*-TiO_{2-x} domain, respectively. In contrast, the Pt metal
17 cannot create the blocking layer such as Pt-Ti-O, even though it has a little power
18 gathering oxygen ions from the titanium oxide layer. However, the oxygen ions
19 continuously diffuse out to a surface through a grain boundary until the thickness of Pt
20 reaches at a critical point, making the *a*-TiO₂ film more oxygen-deficient *a*-TiO_{2-x}. The
21 light contrast, shown in Figure 2d, indicates this phenomenon. As expected, the Mo top
22 electrode, whose oxygen affinity is a value between the Al and Pt, exhibited an
23 intermediate contrast, as shown in Figure 2c.

24 In summary, we have investigated the influence of top metal electrodes on the
25 resistive switching properties in Metal/TiO₂/Al devices. Although the all devices showed

1 BRS behaviors, the higher on/off resistance ratio could be obtained in the Al top metal
2 case with the lowest oxide formation energy. The highest oxygen affinity induced the
3 strong interaction between top metal electrode and the top domain of TiO₂ at the initial
4 stage of metal deposition process, thus creating newly formed interface layer, as confirmed
5 by HRTEM images and STEM EDS analysis. On the base of these results, it is strongly
6 demonstrated the switching behaviors of metal/TiO₂/Al memory devices depend on the
7 interface reaction with top metal electrodes rather than a work function.

8 9 **Acknowledgments**

10 This work was supported by the Next-generation Non-volatile Memory Program of
11 the Ministry of Knowledge Economy (10029953-2009-31) and the Korea Research
12 Foundation Grant (MOEHRD) (KRF-2008-005-J00902). The authors sincerely thank the
13 technical staffs of the Process Development Team at ETRI for their support with the
14 PEALD facility.

1 **References**

2 ¹M.-J. Lee, S. I. Kim, C. B. Lee, H. Yin, S.-E. Ahn, B. S. Kang, K. H. Kim, J. C. Park, C. J.
3 Kim, I. Song, S. W. Kim, G. Stefanovich, J. H. Lee, S. J. Chung, Y. H. Kim, Y. Park, Adv.
4 Funct. Mater. **19**, 1587 (2009).

5 ²J. J. Yang, M. D. Pickett, X. Li, D. A. A. Ohlberg, D. R. Stewart, and R. S. Williams
6 Nature Nanotech. **3**, 429 (2008).

7 ³Y. C. Yang, F. Pan, Q. Liu, M. Liu, and F. Zeng Nano Lett. **9**, 1636 (2009).

8 ⁴M.-J. Lee, S. Han, S. H. Jeon, B. H. Park, B. S. Kang, S.-E. Ahn, K. H. Kim, C. B. Lee, C.
9 J. Kim, I.-K. Yoo, D. H. Seo, X.-S. Li, J.-B. Park, J.-H. Lee, and Y. Park, Nano Lett. **9**,
10 1476 (2009).

11 ⁵D.-H. Kwon, K. M. Kim, J. H. Jang, J. M. Jeon, M. H. Lee, G. H. Kim, X.-S. Li, G.-S.
12 Park, B. Lee, S. Han, M. Kim, and C. S. Hwang, Nature Nanotech. **5**, 148 (2010).

13 ⁶C. B. Lee, B. S. Kang, A. Benayad, M. J. Lee, S.-E. Ahn, K. H. Kim, G. Stefanovich, Y.
14 Park, and I. K. Yoo, Appl. Phys. Lett. **93**, 042115 (2008).

15 ⁷C.-Y. Lin, C.-Y. Wu, C.-Y. Wu, T.-C. Lee, F.-L. Yang, C. Hu, and T.-Y. Tseng, IEEE
16 Electron Device Lett. **28**, 366 (2007).

17 ⁸H. Y. Jeong, J. Y. Lee, M.-K. Ryu, and S.-Y. Choi, Phys. Status Solidi-R **4**, 28 (2010).

18 ⁹H. Y. Jeong, J. Y. Lee, S.-Y. Choi, and J. W. Kim, Appl. Phys. Lett. **95**, 162108 (2009).

19 ¹⁰H. B. Michaelson, IBM J. Res. Develop. **22**, 72 (1978).

20 ¹¹R. Schmiede, V. Demuth, P. Lahnor, H. Godehardt, Y. Bodschwinn, C. Harder, L.
21 Hammer, H.-P. Strunk, M. Schulz, and K. Heinz, Appl. Phys. A **62**, 223 (1996).

22 ¹²W. Shen, R. Dittmann, U. Breuer, and R. Waser, Appl. Phys. Lett. **93**, 222102 (2008).

23

24

25

1 **Figure Captions**

2 FIG. 1. (Color online) (a) Typical J-V curves of Al (Cr, Mo, W, and Pt)/TiO₂/Al. The right
3 below inset shows a schematic diagram of our crossbar type memory with 60 μm ×60 μm
4 (3600 μm²). (b) J-V characteristics of Metal/TiO₂/Al devices in a double-logarithmic plot.
5 The colored values mean the slopes of linear fitting of each separated regions.

6

7 FIG. 2. (Color online) Cross-sectional HRTEM images with the same magnification of (a)
8 TiO₂/Al layered structure before the deposition of top metal electrodes, (b) Al/TiO₂/Al
9 device, (c) Mo/TiO₂/Al, ad (d) Pt/TiO₂/Al. The red dot lines have all the same width in the
10 each figure to compare interface changes after deposition of top metal electrodes.

11

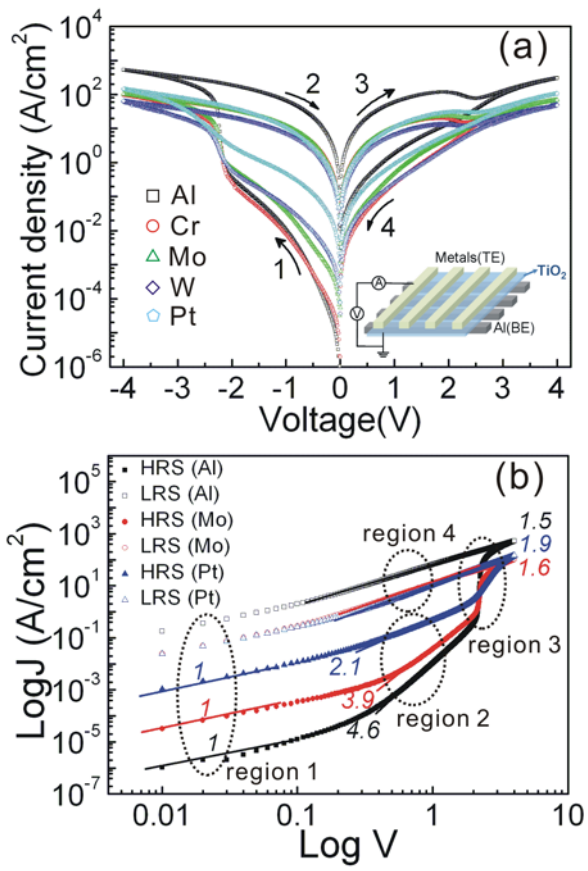
12 FIG. 3. (Color online) Cross-sectional annular dark field (ADF) STEM Z-contrast image of
13 (a) *a*-TiO₂/Si, (b) Al/*a*-TiO₂/Si, and (c) Pt/*a*-TiO₂/Si samples. The point EDS spectra are
14 shown in the right inset of (a), (b) and (c). The line profile of each sample are displayed in
15 (d), (e), and (f), respectively.

16

17 FIG. 4. (Color online) Schematic illustration showing the different phenomena occurred at
18 the top interface region during Al ((a) and (b)) and Pt ((c) and (d)) top metal deposition.

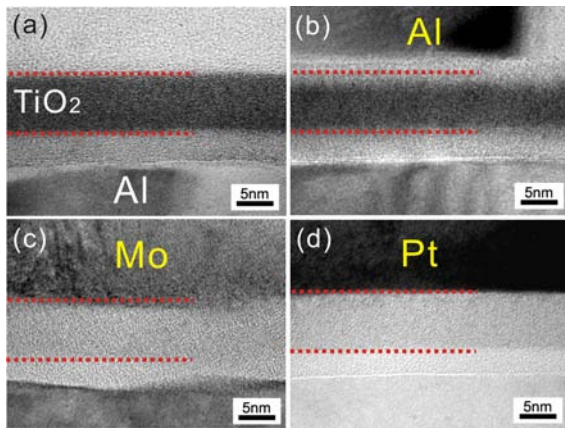
19

1 Figure 1. (Jeon et al.)



2
3
4

1 Figure 2. (Jeon et al.)

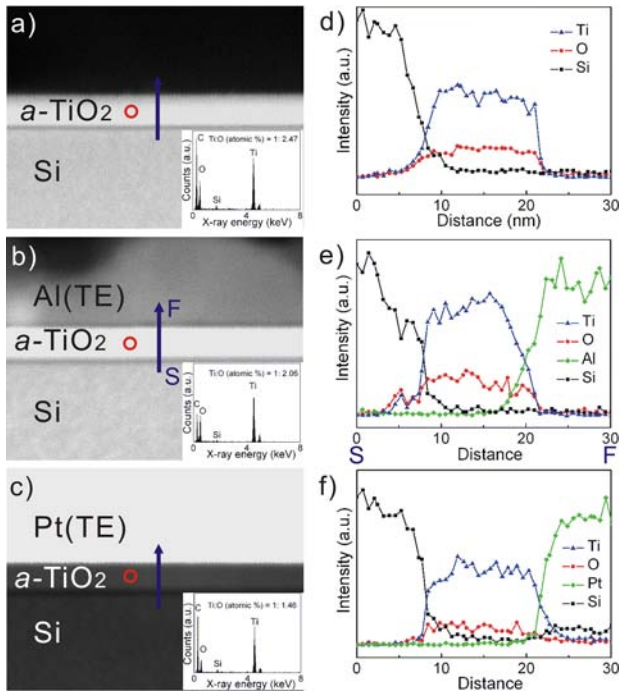


2

3

4

1 Figure 3. (Jeon et al.)

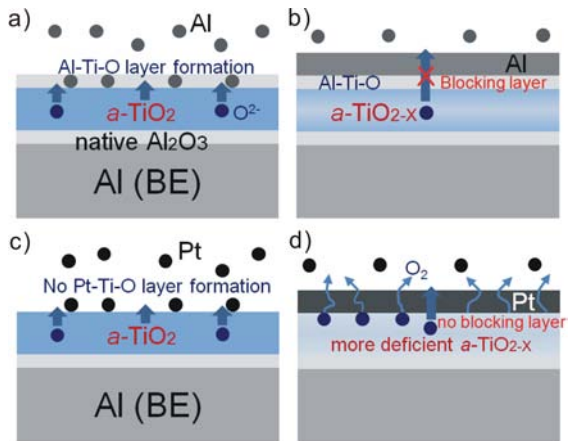


2

3

4

1 Figure 4. (Jeon et al.)



2

3